A New Method of Characterizing Material Viscoelastic Property by Using Vector Fitting

Huimin Li,[1] Boming Zhang,[1] Guanghui Bai[2]
[1]*Materials Science and Engineering School, Beihang University, Beijing, People's Republic of China*

[2]*Beijing Institute of Near Space Flight Vehicle Systems Engineering, Beijing, People's Republic of China*

A numerical algorithm is first established to characterize viscoelastic properties of materials by using vector fitting which is used more commonly for system identification in the field of electronic and automatic control. Combining with correspondence principle, the present numerical algorithm is employed to predict the viscoelastic properties of no-flow underfill material. The predicted results are compared with the experiment data. Very good agreement between numerical algorithm and experiment results is illustrated for the materials. As the form is simple, the relaxation modulus can be easily switched from frequency domain to time domain by using inverse Laplace transformation. The present algorithm can also be used to characterize viscoelastic properties of other materials. POLYM. COMPOS., 00:000–000, 2015. © 2015 Society of Plastics Engineers

INTRODUCTION

Fiber-reinforced polymer matrix composite materials are widely used in the manufacture of composite parts for different applications in industries as diverse as automotive, marine, aerospace, infrastructure, and sports good [1]. Hence, prediction of the mechanical properties of these polymeric composites is absolutely desirable for the design of engineering composite structures from an industrial point of view [2]. A special interest is addressed to the viscoelastic properties and their influence on performance, since polymers or polymer composites are known to exhibit viscoelastic behavior, especially at high temperature and moisture.

Many researchers have devoted considerable effort to characterize viscoelastic properties of composites by using different experiment methods [3–6] and many prediction models have been proposed in the literature during the past 50 years and this trend continues. [7–10] However, the common experiment method of characterizing material viscoelastic properties is using a dynamic mechanical analyzer (DMA) that provides valuable insight into the structure, morphology, and viscoelastic behavior of polymeric materials. Storage modulus gives an insight into the stiffness behavior and load-bearing capability of a composite material, which is a measure of the maximum energy stored in the material during one cycle of oscillation. Loss modulus is proportional to the amount of energy dissipated as heat by the sample [11], [12]. The mechanical damping coefficient is the ratio of the loss modulus to the storage modulus and is related to the degree of molecular mobility in the polymeric material [13], [14]. The experiments include stress relaxation, [15], [16], creep, [17–19], and dynamic mechanical analysis using multiple fixed frequencies [20–26]. The relaxation process of polymer is slow and needs longer time for experimental observation at low temperature. However, it is fast and requires shorter time for experimental measure. The temperature range used in acquiring the data determines the breadth of time span covered in the master curve. By using the time/temperature superposition (TTS) principle which assumes changing the experimental temperature has the same effect as changing the relaxation time, a master curve at an arbitrary reference temperature that extends the mechanical measurement (i.e., modulus or compliance) beyond the range of laboratory scale in either the time or the frequency domain can be constructed. The Williams–Landel–Ferry (WLF) equation [27], [28] and Arrhenius equation are usually used to analyze the viscoelastic data [29]. The advantage of dynamic mechanical analysis using multiple fixed frequencies is the limited frequency range provided by the apparatus could be compensated by use of a wider temperature range, as long as the TTS principle is still applicable in the temperature range of interest. In other words, if the accessible temperature range is limited, a wider frequency range should be used for obtaining experimental data to construct a complete master curve. When the master curves in the frequency domain are established, it is necessary to know the relaxation modulus in the time domain during the process of predicting stress using a finite

Correspondence to: H. Li; e-mail: fengyun327@163.com
DOI 10.1002/pc.23359
Published online in Wiley Online Library (wileyonlinelibrary.com).

element analysis technique. Several approximated equations are used to estimate the relaxation modulus. The one suggested by Schwarzl and Struik is given as [25], [30]:

$$E(1.25t)=E'(\omega)-0.5303E''(0.5282\omega) \\ -0.021E''(0.085\omega)+0.042E''(6.37\omega) \quad (1)$$

Where $\omega=1/t=2\pi f$, E' and E'' are the master curves determined in the frequency domain.

Another is proposed by Ninomiya and Ferry [31], [32]:

$$E(t)=E'(\omega)-0.4E''(0.4\omega)+0.014E''(10\omega) \quad (2)$$

In order to get the equation of relaxation modulus *E(t)*, both approximated equations need to perform twice data fitting whose errors are accumulated. These processes are also complex.

To resolve these issues, a method of vector fitting which is used more commonly in the field of electronic and automatic control is first established to characterize the viscoelastic properties of materials in this work. Combining with the viscoelastic correspondence principle that shows the analogy between viscoelasticity and linear elasticity, the method of vector fitting is developed. Based on these theories, a numerical algorithm of switching the relaxation modulus from frequency domain to time domain is given. The predicted results of material viscoelastic properties by using this algorithm is compared with experiment data obtained from reference.

CORRESPONDING PRINCIPLE

Under small deformation assumption, the linear viscoelastic constitutive equation for predicting the relaxation of the stress in the composite structures can be expressed by the following hereditary integral:

$$\sigma_{ij}(t)=\int_0^t C_{ijkl}(t-\tau)\frac{d\varepsilon_{kl}}{d\tau}d\tau, i,j,k,l=1,2,3 \quad (3)$$

Where, C_{ijkl} is the material stiffness tensor.

Taking the Laplace transform of *Eq. 3*, constitutive equation for such a material in the image domain can be gotten as follows:

$$\hat{\sigma}_{ij}(s)=s\hat{C}_{ijkl}(s)\hat{\varepsilon}_{kl}(s) \quad (4)$$

which shows the analogy between viscoelasticity and linear elasticity, if the transformed viscoelastic material function $s\hat{C}_{ijkl}(s)$ in the image domain is interpreted as an elastic material parameter C:

$$s\hat{C}_{ijkl}(s) \Longleftrightarrow C \quad (5)$$

This is the basis for the correspondence principle, which states that a VE problem is equivalent to a corresponding elastic problem. [33] The moduli can be found from the above equation.

VECTOR FITTING

Vector fitting (VF) which is first proposed by Gustavsen and Semlyen [34] and then improved by Gustavsen [35] and Deschrijver et al. [36] has become a popular tool for system identification of linear systems in the frequency domain. The application has typically been the modeling of devices and subsystems for the purpose of transient analysis in power systems and signal integrity characterization of microwave systems. VF has also been used for shielding analysis in electromagnetic-compatibility (EMC) studies, Green's functions representation, and optimal sample calculations [35]. However, papers on the application of VF technology in the field of material science have not been seen. In this section, we start by reviewing the formulation of VF and then introduce its application in material science.

Vector Fitting

In principle, an approximation of a given order can be found by fitting a ratio of two polynomials to the data of transfer function:

$$f(s)=\frac{\sum_{i=1}^{N} a_i s^i}{\sum_{i=1}^{N} b_i s^i} \quad (6)$$

By multiplying both sides with the denominator, *Eq. 6* can be rewritten as a linear problem:

$$Ax=b \quad (7)$$

However, the resulting problem is badly scaled and conditioned as the columns in A are multiplied with different powers of s. This limits the method to approximations of very low order, particularly if the fitting is over a wide frequency range.

In order to overcome the shortcoming, the frequency response $f(s)$ is approximated with a rational function:

$$f(s)=\sum_{n=1}^{N}\frac{r_n}{s-a_n}+d+h\cdot s \quad (8)$$

Where, the residues r_n and poles p_n are either real quantities or come in complex conjugate pairs, while d and h are real and optional.

As explained in [34], [35], the VF first identifies the poles of $f(s)$ by solving in the least squares sense, the linear problem

$$\sigma(s)f(s)=q(s) \quad (9)$$

Where

 DOI 10.1002/pc

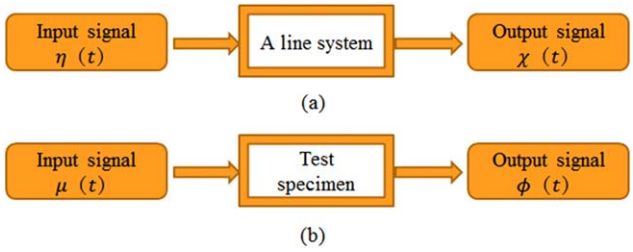

FIG. 1. The schematic diagram of testing processes. [Color figure can be viewed in the online issue, which is available at wileyonlinelibrary.com.]

$$\sigma(s)=\sum_{m=1}^{N}\frac{r_{\mathrm{m}}}{s-p_{\mathrm{m}}}+1 \tag{10}$$

$$q(s)=\sum_{m=1}^{N}\frac{\widehat{r}_{\mathrm{m}}}{s-p_{\mathrm{m}}}+d+h\cdot s \tag{11}$$

Where $\sigma(s)$ is a scalar while $q(s)$ is generally a vector, and p_{m} is a set of initial poles.

A rational function approximation for $f(s)$ can now be readily obtained from*Eq. 9*. This becomes evident if each sum of partial fractions in *Eq. 10* is written as a fraction:

$$\sigma(s)=\frac{\prod_{m=1}^{N}(s-z_{\mathrm{m}})}{\prod_{m=1}^{N}(s-p_{\mathrm{m}})},\ q(s)=h\frac{\prod_{m=1}^{N+1}(s-\bar{z}_{\mathrm{m}})}{\prod_{m=1}^{N}(s-p_{\mathrm{m}})} \tag{12}$$

Then, we can get

$$f(s)=h\frac{\prod_{m=1}^{N+1}(s-\bar{z}_{\mathrm{m}})}{\prod_{m=1}^{N}(s-z_{\mathrm{m}})} \tag{13}$$

It can then be seen that the poles of $f(s)$ must be equal to the zeros of $\sigma(s)$ which can be calculated as the eigen values of a matrix [28]

$$\{a_n\}=eig(A-b\cdot c^{T}) \tag{14}$$

Where A is a diagonal matrix holding the initial poles p_{m}, b is a column vector of ones and c^{T} is a row vector holding the residues z_{m}.

The procedure can be applied in an iterative manner where *Eq. 9* and *Eq. 14* are solved repeatedly with the new poles replacing the previous poles. This pole relocation procedure usually converges in 2–3 iterations. After the poles have been identified, the residues of *Eq. 8* are finally calculated by solving the corresponding least-squares problem with known poles.

Application in Material Science

In the field of automatic control, the line system transfer function $f(s)$ which is systematically inherent attribute is obtained by input signal $\eta(s)$ and the corresponding response $\chi(s)$, as shown in Fig. 1a. The expression is as follows:

$$f(s)=\frac{\chi(s)}{\eta(s)} \tag{15}$$

In the DMA test, the material property $E(s)$ which is also material inherent nature is obtained by using the input signal $\phi(s)$ and output signal $\mu(s)$, as shown in Fig. 1b. The material property is expressed as follows:

$$E(s)=\frac{\phi(s)}{\mu(s)} \tag{16}$$

Both *Eqs. 15* and *16* are similar. Therefore, VF technology can be used for materials characterization.

Master curves in the frequency domain can be generated by shifting the storage and loss moduli which is obtained by dynamic mechanical analysis using multiple fixed frequencies. Relaxation modulus is written as following in the frequency domain:

$$E(\omega)=E'(\omega)+iE''(\omega) \tag{17}$$

Where $E(\omega)$ is relaxation modulus, $E'(\omega)$ and $E''(\omega)$ are the storage and loss modulus, respectively.

The expression of relaxation modulus that is similar to transfer function in the field of automatic control can be gotten by using VF technology in the frequency domain.

$$E(s)=\sum_{n=1}^{N}\frac{r_{\mathrm{n}}}{s-a_{\mathrm{n}}}+d \tag{18}$$

We can rewrite the *Eq. 18* as follows:

$$E(s)=\sum_{n=1}^{N}\frac{s\cdot\tilde{r}_{\mathrm{n}}}{s-a_{\mathrm{n}}}+\tilde{d} \tag{19}$$

Applying the corresponding principle and inverse Laplace transformation technique, relaxation modulus formula in time domain can be obtained.

$$E(t)=\ell^{-1}\left(\frac{E(s)}{s}\right)=\tilde{d}+\sum_{n=1}^{N}\tilde{r}_{\mathrm{n}}\cdot e^{a_{\mathrm{n}}t} \tag{20}$$

Where $\ell^{-1}(\cdot)$ is inverse Laplace transformation.

VERIFICATION

Experiment Data

No-flow underfill is an alternative material technology for packaging high-speed flip-chip assemblies in microelectronics industry. The no-flow underfill material contains hardeners, silica filler, coupling agent, fluxing agent, and other additives. By conducting the time–temperature superposition (TTS) experiments using DMA, He [18] has

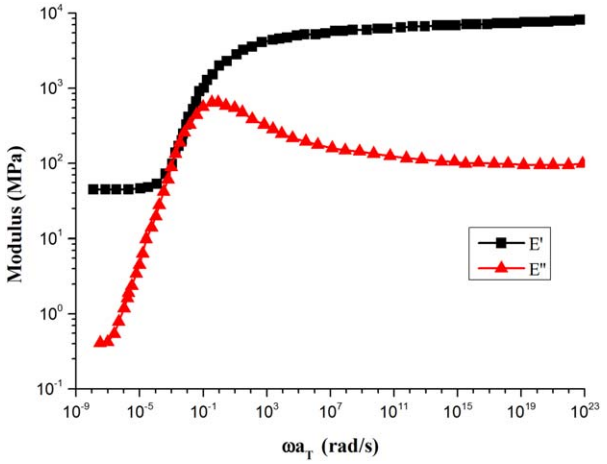

FIG. 2. Master curves generated by shifting the storage and the loss moduli using the TTS principle with respect to a reference temperature of 100°C. [10]. [Color figure can be viewed in the online issue, which is available at wileyonlinelibrary.com.]

presented master curves of no-flow underfill material for both the storage and loss moduli as a function of frequency at a preselected reference temperature as shown in Fig. 2. The material is selected because the experiment data in the literature is sufficient to verify the algorithm. However, the algorithm can be used to characterize viscoelastic properties of other materials but not just confined to this material.

Verification

In this section, relaxation modulus is first approximated by using VF, based on the experiment master curves data. Then, the predicted result of relaxation modulus is compared with results obtained from the stress relaxation experiments.

Result of VF. Figure 3 shows the resulting fitting by the VF when using 18 poles and 3 iterations. Solid

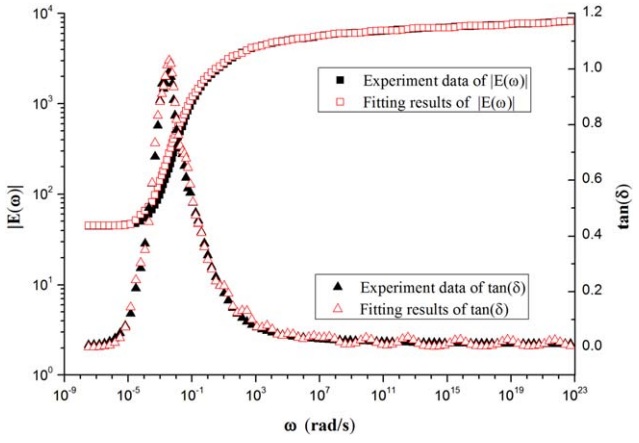

FIG. 3. Eighteenth order approximation of *E(s)* after three iterations. [Color figure can be viewed in the online issue, which is available at wileyonlinelibrary.com.]

TABLE 1. Results of VF fitting for *Eq. 18*..

Poles (a_n)	Residues (r_n)	Poles (a_n)	Residues (r_n)
−5.009E + 21	−2.103E + 24	−2.630E + 02	−2.241E + 05
−6.761E + 18	−2.839E + 21	−1.452E + 01	−1.391E + 04
−5.434E + 15	−2.200E + 18	−1.187E + 00	−2.616E + 03
−3.135E + 12	−1.487E + 15	−7.683E − 01	4.622E + 03
−9.162E + 09	−3.806E + 12	−6.422E − 01	−3.255E + 03
−4.921E + 07	−1.838E + 10	−6.810E − 02	−4.773E + 01
−3.728E + 06	−1.331E + 09	−8.288E − 03	−3.046E + 00
−1.510E + 05	−6.484E + 07	−9.942E − 04	−7.205E − 02
−5.978E + 03	−3.536E + 06	−5.072E − 05	−9.515E − 04
$N = 18$		$d = 8156.414$	

squares and triangles are magnitude and loss tangent (*tanδ*) of relaxation modulus obtained from experiment, respectively. Open squares and triangles are the VF results of the two, respectively. From Fig. 3, we can observe that both predicted master curve and loss tangent curve are in good agreement with the obtained experiment master curves. The VF results of *Eq. 18* are listed in Table 1.

Then, the coefficients of *Eq. 19* are obtained by rewriting the *Eq. 18*, listed in Table 2. Applying the corresponding principle and inverse Laplace transformation technique to *Eq. 19*, relaxation modulus *E(t)* in time domain is obtained.

$$E(t) = \tilde{d} + \sum_{n=1}^{N} \tilde{r}_n \cdot e^{a_n t} \tag{21}$$

Compared with the Stress Relaxation Experiments. An approach to construct the master curve for relaxation modulus in the time domain is to conduct stress relaxation experiments at various isothermal temperatures. The master curve for *E(t)* in the time domain is given in reference [18] by shifting each isothermal curve of *E* versus *t* with respect to a reference temperature, using the same TTS principle, as shown in Fig. 4. The calculated relaxation moduli predicted by using *Eq. 21*, *Eqs. 1* and *2* are also plotted in Fig. 4. The solid squares and circles are the experiment data and the VF predicted results,

TABLE 2. Results of coefficient fitting for *Eq. 19*..

Poles(a_n)	Residues($\tilde{r}_n$)	Poles(a_n)	Residues($\tilde{r}_n$)
−5.009E + 21	5.311E + 02	−2.630E + 02	7.805E + 02
−6.761E + 18	4.020E + 02	−1.452E + 01	1.310E + 03
−5.434E + 15	3.953E + 02	−1.187E + 00	−2.911E + 03
−3.135E + 12	5.036E + 02	−7.683E − 01	8.593E + 03
−9.162E + 09	3.918E + 02	−6.422E − 01	−4.940E + 03
−4.921E + 07	3.393E + 02	−6.810E − 02	9.950E + 02
−3.728E + 06	4.279E + 02	−8.288E − 03	3.757E + 02
−1.510E + 05	3.319E + 02	−9.942E − 04	7.051E + 01
−5.978E + 03	6.117E + 02	−5.072E − 05	−3.464E + 00
$N = 18$		$\tilde{d} = 45.038$	

DOI 10.1002/pc

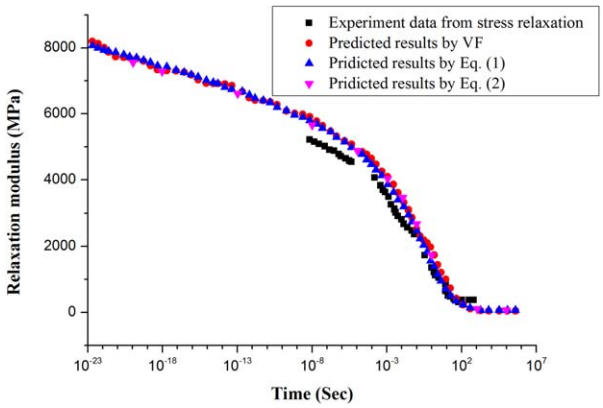

FIG. 4. Predicted results of relaxation modulus. [Color figure can be viewed in the online issue, which is available at wileyonlinelibrary.com.]

respectively. The solid triangles are the calculated results of *Eqs. 1* and *2*. They agree very well with the results obtained using *Eq. 21* and so does the experiment master curve.

In reference [18], the author gives experimentally obtained relaxation modulus data, which are from two independent measurements on two different samples. In Fig. 5, the relaxation modulus data obtained from the reference are plotted together with the relaxation modulus calculated using *Eqs. 1* and *19*. The lines with open triangles and circles are the two experiment data, respectively. The lines with solid triangles are the predicted results using *Eqs. 1* and *21*, respectively. It can be observed the predicted results by VF are fairly good agreement with the experiment data.

DISCUSSION

Mechanical properties of the viscoelastic polymers are time dependent. The degree of change in the mechanical properties of polymeric materials over time depends on many factors. These are primarily the temperature, pressure, humidity, plasticizing effect, and stress conditions to which the material is subjected during its manufacture and during its application. [8] However, the characterization of polymer viscoelastic properties is usually by means of DMA experiments under certain conditions. When performing multiple-frequency DMA experiments, an important problem is the conversion of master curve expression between frequency domain and time domain, since expressions used in numerical methods of predicting material behavior is usually the expressions in time domain. The predicted results of approximated equations are not ideal, as shown in Fig. 5. And, the implementation processes of these equations are also complicated. However, it is a good way to avoid these problems by using VF technology. The VF technique is a robust macromodel for efficient time domain and frequency domain simulation which circumvents the ill-conditioning and unbalanced weighting problems that usually exist in a rational approximation problem. However, VF still suffers from computationally inefficiency if the studied has a relatively large number of ports. [37]. Deschrijver et al. [36] presents a robust approach that removes the sparsity of the block-structured least-squares equations by a direct application of the QR decomposition. In material science, relaxation moduli of materials are approximated in frequency by using VF technique. Then, applying the corresponding principle and inverse Laplace transformation technique, relaxation modulus formula in time domain can be obtained. The advantage of this method is the relaxation modulus can be fitted more accurately if appropriate N is chosen in frequency domain. As the form is simple, the relaxation modulus in frequency domain can be easily switched to that in time domain by using inverse Laplace transformation.

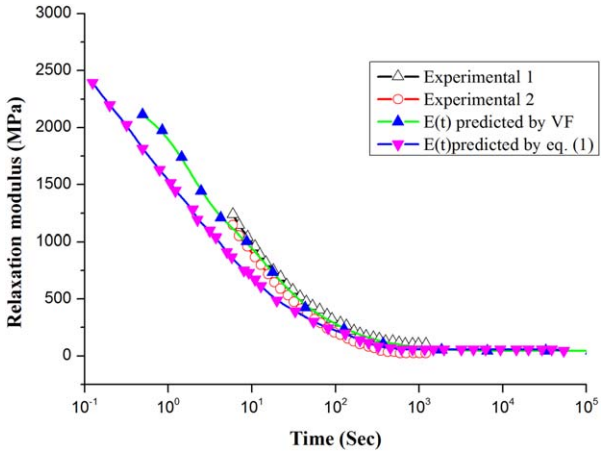

FIG. 5. Predicted results of relaxation modulus and two independent stress relaxation experiment results. [Color figure can be viewed in the online issue, which is available at wileyonlinelibrary.com.]

CONCLUSION

This study extends the method of vector fitting from the field of electronic and automatic control to characterizing material viscoelastic properties in material science. Using correspondence principle, a numerical algorithm of switching the relaxation modulus from frequency domain to time domain is established. This algorithm is validated by using experiment data. Very good agreement between numerical algorithm and the experiment data is illustrated for the viscoelastic properties of no-flow underfill materials. The present algorithm can also be used to characterize viscoelastic properties of other materials.

REFERENCES

1. A.A. Somashekar, S. Bickerton, D. Bhattacharyya, *Composites. Part A.*, **43**, 1044 (2012).
2. C. Cruz, J. Diani, and G. Régnier, *Composites. Part A.*, **40**, 695 (2009).
3. A. Zhang, H. Lu, and D. Zhang, *Polym. Compos.*, DOI: 10.1002/pc.23149.

4. P. Dasappa, P. Lee-Sullivan, X. Xiao, and P.H. Foss, *Polym. Compos.*, **30**, 1146 (2009).
5. E.M. Woo, J.C. Seferis, and R.S. Schaffnit, *Polym. Compos.*, **12**, 273 (1991).
6. H. Luo, G. Lu, S. Roy, and H. Lu, *Mech. Time-Depend. Mater.*, **17**, 369 (2013).
7. H. Lu, W.M. Huang, and J. Leng, *Smart. Mater. Struct.*, **23** (2014).
8. H. Li, and B. Zhang, *Int. J. Plast.*, **65**, 22 (2015).
9. H. Lu, and W.M. Huang, *Smart. Mater. Struct.*, **22** (2013).
10. H. Lu, and S. Du, *Polym. Chem.*, **5**, 1155 (2014).
11. G. Gong, J. Pyo, and A.P. Mathew, K. Oksman. *Composites., Part A.* **42**, 1275 (2011).
12. B. Baghaei, M. Skrifvars, M. Salehi, T. Basir, M. Rissanen, and P. Nousiainen, *Composites. Part A.*, **61**, 1 (2014).
13. G. Gejo, T.E. Jose, A. Dan, S. Mikael, E.R. Nagarajan, J. Kuruvilla, *Composites. Part A.*, **43**, 893 (2012).
14. P.V. Joseph, G. Mathew, K. Joseph, G. Groeninckx, and S. Thomas, *Composites. Part A.*, **34**, 275 (2003).
15. Kim, K. Yeong, and R. Scott, *Polym. Eng. Sci.*, **36**, 2852 (1996).
16. R.W. Scott, and Y.K. Kim, *Mech. Compos. Mater. Struct.*, **5**, 153 (1998).
17. H. Luo, G. Lu, S. Roy, and H. Lu, *Mech. Time-Depend. Mater.*, **17**, 369 (2013).
18. H. Yi, *Thermochim. Acta.*, **439**, 127 (2005).
19. S.R. White, and A.B. Hartman, *J. Eng. Mater. Technol.*, **119**, 262 (1997).
20. E.M. Woo, J.C. Seferis, and R.S. Schaffnit, *Polym. Compos.*, **12**, 273 (1991).
21. M. Sadeghinia, K.M.B. Jansen, and L.J. Ernst, *Microelectron Reliab.*, **52**, 1711 (2012).
22. Montazeri, Arash, K. Pourshamsian, and M. Riazian, *Mater. Design.*, **36**, 408 (2012).
23. M. Sadeghinia, K.M.B. Jansen, and L.J. Ernst, *Int. J. Adhes. Adhes.*, **32**, 82 (2012).
24. Guo, Jiaxi, L. Grassia, and S.L. Simon, *J. Polym. Sci., Part B: Polym. Phys.*, **50**, 1233 (2012).
25. O'Brien, J. Daniel, P.T. Mather, and S.R. White, *J. Compos Mater.*, **35**, 883 (2001).
26. Simon, L. Sindee, G.B. Mckenna, and O. Sindt, *J. Appl. Polym. Sci.*, **76**, 495 (2000).
27. J.D. Ferry, Viscoelastic Properties of Polymers, 3rd ed., Wiley, New York, (1980).
28. Williams, L. Malcolm, R.F. Landel, and J.D. Ferry, *J. Am. Chem. Soc.*, **77**, 3701 (1955).
29. M.H.H. Meuwissen, H.A. de Boer, H.L.A.H. Steijvers, K.M.B. Jansen, P.J.G. Schreurs, and M.G.D. Geers, *Int. J. Adhes. Adhes.*, **26**, 212 (2006).
30. F.R. Schwarzl, and L.C.E. Struik, *Adv. Mol. Relaxat. Process.*, **1**, 201 (1967).
31. Ninomiya, Kazuhiko, and J.D. Ferry, *J. Colloid. Sci.*, **14**, 36 (1959).
32. K.P. Menard, Dynamic Mechanical Analysis: A Practical Introduction, CRC Press, Boca Raton (1999).
33. A. Matzenmiller, and S. Gerlach, *Comput. Mater. Sci.*, **29**, 283 (2004).
34. B. Gustavsen, and A. Semlyen, *IEEE Trans. Power Delivery.*, **14**, 1052 (1999).
35. B. Gustavsen, *IEEE Trans. Power Delivery.*, **21**, 1587 (2006).
36. D. Deschrijver, M. Mrozowski, T. Dhaene, and D.D. Zutter, *IEEE Microw. Wirel. Compon. Lett.*, **18**, 383 (2008).
37. S. Grivet-Talocia, A. Ubolli, *IEEE Trans. Adv. Packag.*, **29**, 39 (2006).

 DOI 10.1002/pc